



Short communication

Boron doped lithium trivanadate as a cathode material for an enhanced rechargeable lithium ion batteries

Yan Feng, Yali Li*, Feng Hou

Key Laboratory of Advanced Ceramics and Machining Technique, School of Material Science and Engineering, Tianjin University, 92# Weijin Road, Tianjin 30072, PR China

ARTICLE INFO

Article history:

Received 8 July 2008

Accepted 25 October 2008

Available online 6 November 2008

Keywords:

LiV₃O₈

Cathode materials

Boron doping

Lithium-ion battery

ABSTRACT

Boron was doped into lithium trivanadate through an aqueous reaction process followed by heating at 100 °C. The B-LiV₃O₈ materials as a cathode in lithium batteries exhibits a specific discharge capacity of 269.4 mAh g⁻¹ at first cycle and remains 232.5 mAh g⁻¹ at cycle 100, at a current density of 150 mAh g⁻¹ in the voltage range of 1.8–4.0 V. The B-LiV₃O₈ materials show excellent stability, with the retention of 86.30% after 100 cycles. These result values are higher than those previous reports indicating B-LiV₃O₈ prepared by our synthesis method is a promising candidate as cathode material for rechargeable lithium batteries. The enhanced discharge capacities and their stabilities indicate that boron atoms promote lithium transferring and intercalating/deintercalating during the electrochemical processes and improve the electrochemical performance of LiV₃O₈ cathode.

© 2008 Elsevier B.V. All rights reserved.

1. Introduction

Lithium vanadium oxides have been extensively studied as a potential cathode material for lithium ion batteries because of their high specific energy density, high working voltage and long cycle life. These performances, in addition to their low cost and non-toxicity, make the materials a promising alternative to the expensive and toxic LiCoO₂ cathode materials commercially used presently [1]. Of the families of lithium vanadium oxides, the LiV₃O₈ phase is particularly noticeable in the past 20 years because this phase has a high capacity, can be readily fabricated, and has excellent stabilities against oxidation [2–4].

For the successful application of LiV₃O₈ as a cathode in lithium ion batteries, the discharge capacity and cycle ability of LiV₃O₈ remains awaiting to be increased. Studies show that the electrochemical properties, including discharge capacity, rate capacity, and cycle performance, strongly depend on the methods of materials fabrication and processing [5,6]. This motivates extensive efforts in the development of synthesis methods such as the sol–gel method [7,8], hydrothermal reactions [9], flame synthesis [10], and post-processing techniques like grinding [11] and ultrasonic treatment [12].

However, an important approach to enhanced charging performance is the substitution of lithium with other cations. To date, various cations were doped into LiV₃O₈ including Na [13], K [14], Mo

[15], Si [16], Y [17], Mn and Ni [18]. Some are coupled with coating of electronically conductive polymers such as polypyrrole [19,20]. Studies show that doping foreign atoms enhanced the electrochemical performance of lithium batteries. For example, LiSi_{0.05}V₃O₈ remained 224.3 mAh g⁻¹ at cycle 150 and 143.0 mAh g⁻¹ at cycle 300 at a current density of 150 mAh g⁻¹ in the voltage range of 1.8–4.0 V which was higher than undoped LiV₃O₈ [16]. The discharge capacities of LiY_{0.1}V₃O₈ electrode were higher than those of LiV₃O₈ electrode, and the capacity retention at room temperature was higher (0.48% capacity loss/cycle) for LiY_{0.1}V₃O₈ electrode compared to LiV₃O₈ electrode (1.46% capacity loss/cycle) [17].

The enhanced performance from doping is due to enlarged crystal layers which provide good channels for lithium transfer to intercalation/deintercalation in material electrodes. However, over doping may cause poor stability because the main structure of LiV₃O₈ will be destroyed by too much doped atoms [16]. So, the appropriate amount of doping will be chosen to attain good electrochemical properties. In addition, different doping element has a different effect on the structures and electrochemical properties of LiV₃O₈ cathode, which tell us the doping element will be carefully chosen.

Boron is electron-defect element. If it is incorporated into LiV₃O₈ with its enough valences orbital, it would provide a stable structure during charge–discharge process. Additionally, the boron ion can occupy the interlayer site of VO₆ octahedrons and VO₅ trigonal bipyramids in LiV₃O₈ structure. The interlayer distance undergoes an expansion with boron doping, leading to a much easier lithium ion intercalation/deintercalation. The discharge capacity and cycle ability of LiV₃O₈ cathode is expected to be enhanced by boron doping.

* Corresponding author. Tel.: +86 22 27403601; fax: +86 22 27402187.
E-mail address: liyali@tju.edu.cn (Y. Li).

In the present work, we incorporated boron into LiV_3O_8 in the aqueous reaction of V_2O_5 and LiOH with the addition of boron simple substance. XRD and XPS analysis found that the expansion of the interlayer spacing of $\text{B-LiV}_3\text{O}_8$ by boron doping and the +3 oxidation state of boron in $\text{B-LiV}_3\text{O}_8$ material, indicating boron is incorporated into the lattice of LiV_3O_8 . Electrochemical measurement shows the enhanced specific discharge capacity and excellent stability.

2. Experimental

Boron containing LiV_3O_8 was prepared from LiOH , V_2O_5 and boron powders in an aqueous solution followed by heating. LiOH and V_2O_5 of a stoichiometric ratio for LiV_3O_8 and boron powders with the atomic ratios of $\text{Li}:\text{V}:\text{B} = 1:3:0$ and $1:3:0.1$ were added into deionized water. The dispersion was fully mixed by magnetic stirring and heated at 80°C for 0.5 h in kept stirring until the formation of an orange viscous gel. The gel was heated at 100°C for 3 h. $\text{B-LiV}_3\text{O}_8$ products were obtained which was grounded into 180 mesh powders. For studying the effects of boron doping, pure LiV_3O_8 was prepared under the identical conditions but without the boron powder addition.

The structures of products were studied using X-ray diffraction (XRD, Rigaku D/MAX-2500v/pc, $\text{CuK}\alpha$), X-ray photoelectron spectroscopy (XPS, PHI-1600), Fourier transform infrared spectrum (FTIR, WQF-510 Beijing Rayleigh, KBr pellets), and scanning electron microscope (SEM, JSM-6700F JEOL).

For electrochemical tests, cathode electrodes were prepared by mixing the active material (LiV_3O_8 or $\text{B-LiV}_3\text{O}_8$), conductive additive (acetylene black) and binder (PTFE) in a weigh ratio of 75:20:5. The materials, as a cathode, were assembled into lithium batteries in an argon filled glove box, with the use of Celgard 2300 as a separator, Li foil counter and reference electrodes, and 1 mol dm^{-3} LiPF_6 in ethylene carbonate (EC), propylene carbonate (PC) and dimethyl carbonate (DMC) (1:1:1 by volume, Jinniu) as electrolyte, to form laboratory-made coin-type cells (size: CR2032).

Galvanostatic charge–discharge cycle tests were performed on a LAND 2001A battery testing system (Wuhan Jinnuo, China) at a current density of 150 mAh g^{-1} in the potential range of 1.8–4.0 V vs. Li^+/Li . Cyclic voltammetry (CV) test was performed on a CHI 660C electrochemical workstation at a scan rate of 0.5 mAh g^{-1} on the potential interval 1.6–4.2 V vs. Li^+/Li . All the tests were performed at room temperature.

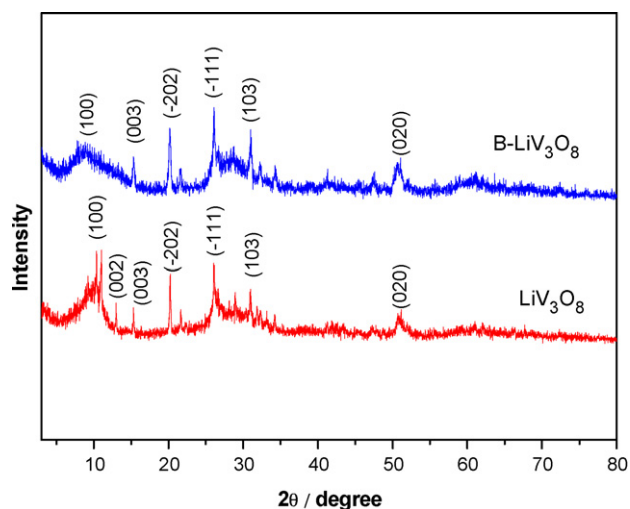


Fig. 1. XRD patterns of LiV_3O_8 and $\text{B-LiV}_3\text{O}_8$.

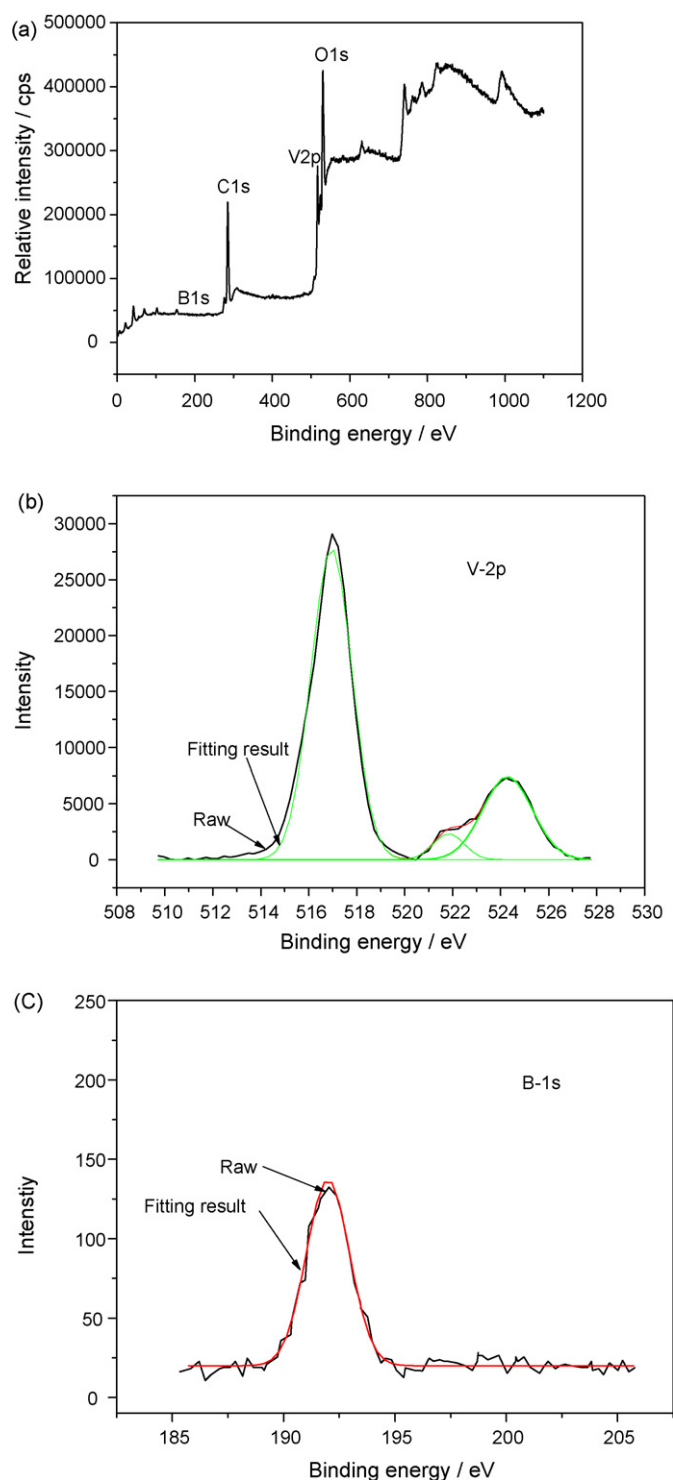


Fig. 2. XPS patterns of $\text{B-LiV}_3\text{O}_8$. (a) XPS survey spectrum; (b) high resolution XPS spectra of V-2p; (c) high resolution XPS spectra of B-1s.

3. Results and discussion

It is known that a lower degree of crystallization of LiV_3O_8 enhances the electrochemical performance [21]. X-ray diffractions show that $\text{B-Li}_{0.1}\text{V}_3\text{O}_8$ was poorly crystallized (Fig. 1). The diffraction peak close to 2 theta at 10° is from (100) planes of LiV_3O_8 , and the lattice parameter is calculated to be $d_{(100)} = 10.35\text{ \AA}$ at $2\theta = 8.54^\circ$. This value is larger than $d_{(100)} = 8.55\text{ \AA}$ at $2\theta = 10.34^\circ$ for

undoped LiV_3O_8 . This may indicate that boron may enter the lattice of LiV_3O_8 to shift the lattice parameter to lower angles and expand the interlayer spacing of LiV_3O_8 . Many studies reported this expansion of the interlayer spacing attributes to the inserting of foreign atom during synthesis process, which provides a good channel and enhanced distribution of the Li^+ ions in the LiV_3O_8 layers [16–18,22].

XPS of V (Fig. 2b) show the binding energies of 516.95 and 524.29 eV which is assigned to V^{+5} . The binding energy 521.84 eV is due to V^{+4} . The peak at 191.99 eV attribute to B^{+3} (Fig. 2c). B changes some of V^{+5} in LiV_3O_8 to V^{+4} with the formation of B^{+3} , which is indicated boron reacted with the reactants and may insert into the lattice of LiV_3O_8 .

FTIR (Fig. 3) shows the presence of $\text{V}=\text{O}$ and $\text{V}-\text{O}-\text{V}$. $-\text{OH}$ is found at 1610, 1552 and 1415 cm^{-1} [23]. In $\text{B-LiV}_3\text{O}_8$, the absorptions at 939, 742, 667 and 534 cm^{-1} are observed [24,25]. In undoped LiV_3O_8 the absorptions appear at 960, 744, 667 and 534 cm^{-1} . In comparison, the first absorptions have difference of 21 cm^{-1} indicating that boron doping shift $\text{V}=\text{O}$ and $\text{V}-\text{O}-\text{V}$ stretching to the red side. This may indicate that boron was bridged with vanadium in the doped phases. Combined with XRD result, boron oxide may form interlayers in $\text{V}-\text{O}$ groups that expands the interlayer spacing.

SEM (Fig. 4) shows the particle sizes of $\text{B-Li}_{0.1}\text{V}_3\text{O}_8$ are between 0.5 to 5 μm . The particle sizes of LiV_3O_8 are between 1 and 10 μm . By boron doping, the size of materials is smaller and have more layer structure than the undoped material that can make an important effect on electrochemical performance of the samples.

The charge–discharge curves of $\text{B-LiV}_3\text{O}_8$ are displayed in Fig. 5 together with those of LiV_3O_8 for comparison. The first cycle discharge specific capacity of $\text{B-LiV}_3\text{O}_8$ is 258.8 mAh g^{-1} which is 37.73% higher than that for LiV_3O_8 (187.9 mAh g^{-1}). The significantly increased discharge capacity indicates the pronounced effects of B-doping on the electrochemical performance of the materials. Moreover, the discharge plateau for $\text{B-LiV}_3\text{O}_8$

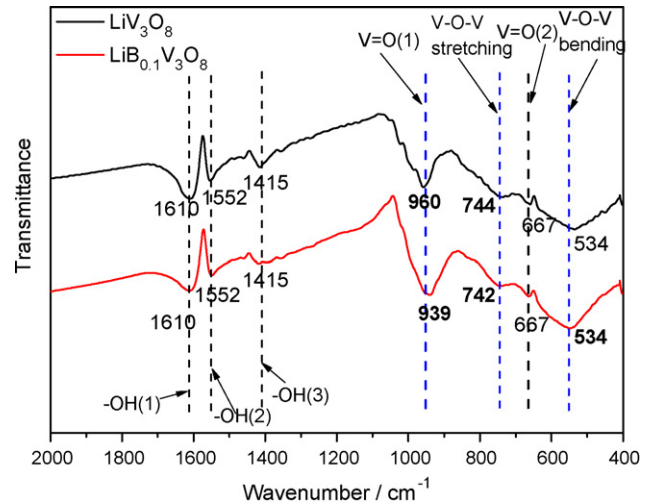


Fig. 3. FTIR spectra of LiV_3O_8 and $\text{B-LiV}_3\text{O}_8$.

is between 2.3 and 2.6 V, and this plateau is absent in the undoping materials. This also benefits from B-doping which Boron oxide may form inter-layers in $\text{V}-\text{O}$ groups making the structure more stable during charge–discharge process. The voltage plateau correspond to cathodic/anodic peaks for the lithium ion intercalation/deintercalation [20]. The voltage plateau is expected because it can ensure the discharge process of battery at a stable voltage range.

Fig. 6 shows charge–discharge cycling of $\text{B-Li}_{0.1}\text{V}_3\text{O}_8$ and LiV_3O_8 . After 100 cycles of charge–discharge, the capacity of $\text{B-Li}_{0.1}\text{V}_3\text{O}_8$ is still over 230 mAh g^{-1} with the capacity retention of 86.30% from the initial value. The capacity after 100 cycles for LiV_3O_8 however increased from 187.9 to 215 mAh g^{-1} . It is interesting to note that

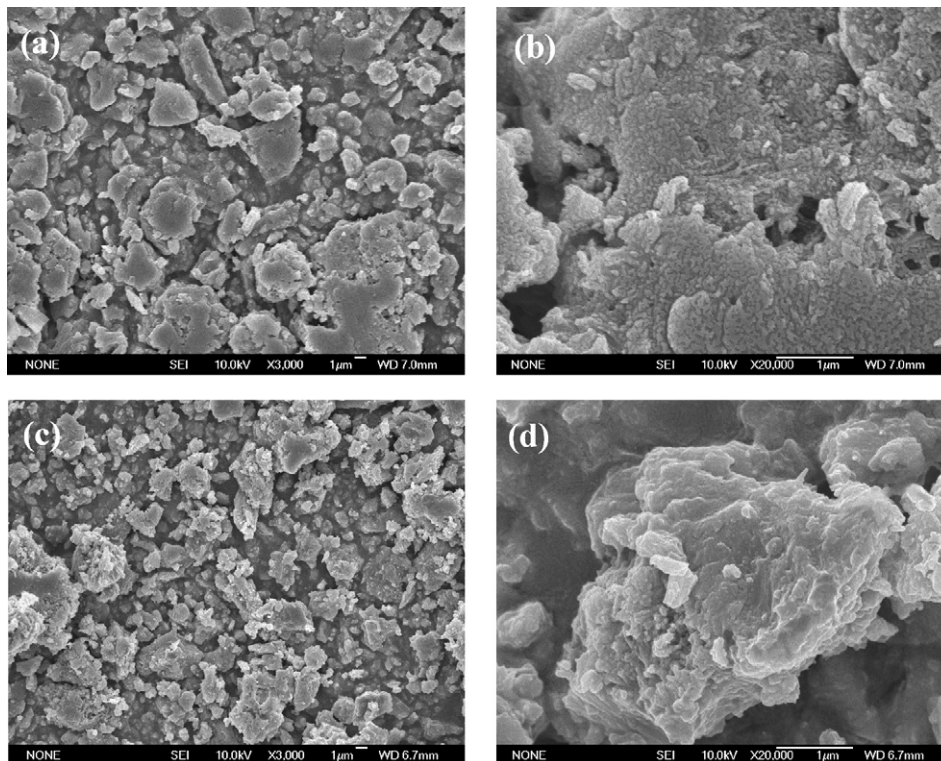


Fig. 4. SEM images of LiV_3O_8 (a, b) and $\text{B-LiV}_3\text{O}_8$ (c, d).

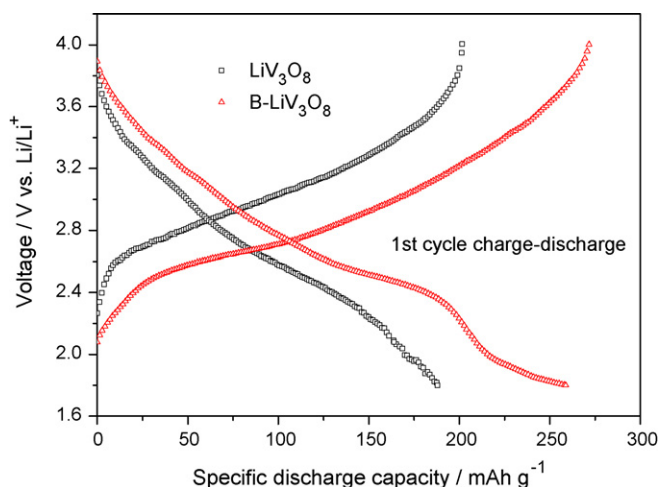


Fig. 5. Initial charge–discharge curves of LiV_3O_8 and $\text{B-LiV}_3\text{O}_8$.

the capacity of $\text{B-LiV}_3\text{O}_8$ still displays a plateau at 228.6 mAh g^{-1} after 83 cycles, while LiV_3O_8 kept absence of this peak value.

The maximum discharge capacity of undoped LiV_3O_8 is shown after some cycles while there is no such expression in $\text{B-LiV}_3\text{O}_8$ material. It is indicated that the diffusivity/intercalation of Li^+ in the undoped LiV_3O_8 is much lower than $\text{B-LiV}_3\text{O}_8$ at the initial stage [20]. It is because by boron doping, the interlayer space is expanded according to XRD result, which provide a good channel and enhanced distribution of the Li^+ ions in the LiV_3O_8 layers. The more diffusion paths of $\text{B-LiV}_3\text{O}_8$ lead to faster intercalation of Li^+ than undoped LiV_3O_8 .

The effects of oxidation of $\text{B-LiV}_3\text{O}_8$ on the CV profiles in a subsequent cycle between 4.0 and 1.8 V are shown in Fig. 7. LiV_3O_8 and the $\text{B-LiV}_3\text{O}_8$ cathode initially have a circuit voltage (OCV) around 3.4 V. The first voltammograms show very different from those reported in literatures [17,18]. The difference is likely resulted from some structural modifications during the first charge and discharge operations. From Fig. 7, it can also be seen that the prolonged cycling kept the shapes of the curves nearly unchanged. This indicates greatly enhanced reversibility of LiV_3O_8 cathode material by B-doping.

Finally, we analyze the second CV curves of $\text{B-LiV}_3\text{O}_8$ and LiV_3O_8 , shown in Fig. 8. The $\text{B-LiV}_3\text{O}_8$ phase show three oxidation peaks at 2.91, 2.44, 3.00 V vs. Li/Li^+ and three reduction peaks at 2.71,

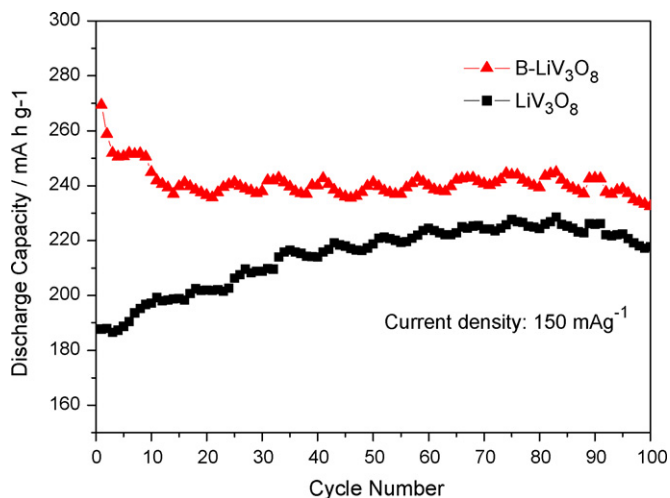


Fig. 6. Cycling stability curves of LiV_3O_8 and $\text{B-LiV}_3\text{O}_8$.

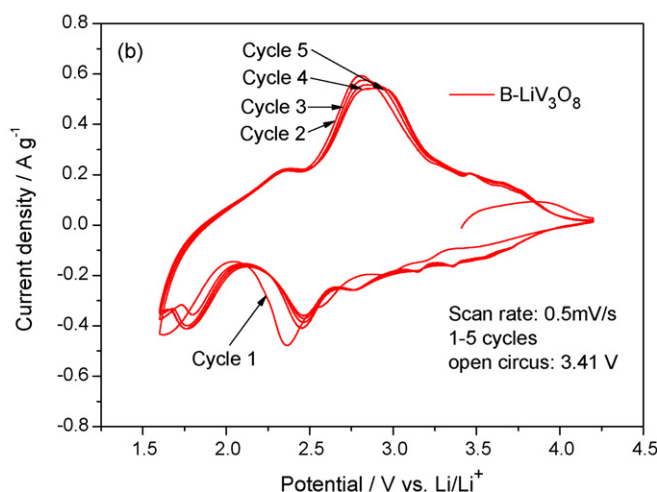
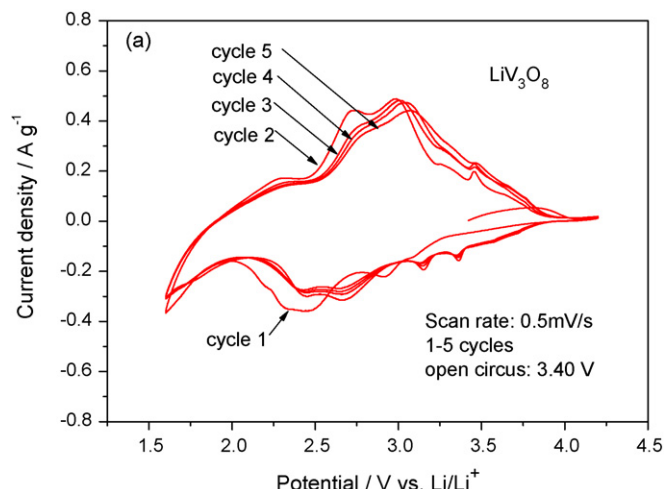


Fig. 7. Cyclic voltammograms of (a) LiV_3O_8 and (b) $\text{B-LiV}_3\text{O}_8$ for 1–5 cycles.

3.01, 3.45 V vs. Li/Li^+ . The boron doped sample exhibits three oxidation peaks at 3.21, 2.98, 2.36 V vs. Li/Li^+ and three reduction peaks at 2.35, 3.47 V vs. Li/Li^+ . The oxidation and reduction peaks of the samples are wide absent of noticeable plateaus. However, B-doping produces a larger peak area than the undoped materials. This indicates a higher specific charge–discharge capacity, in

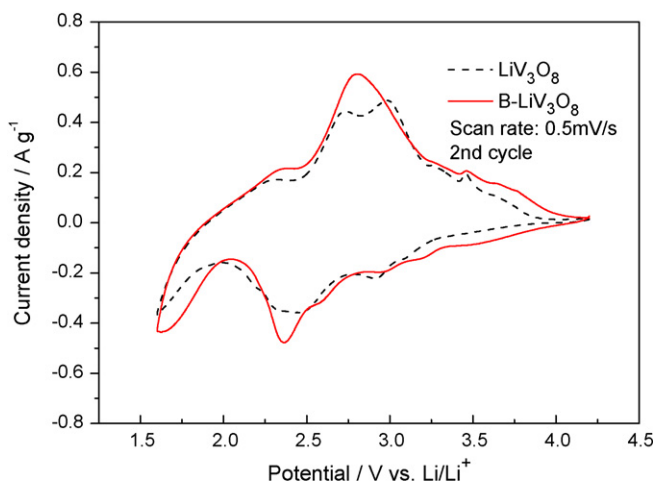


Fig. 8. Cyclic voltammograms of LiV_3O_8 and $\text{B-LiV}_3\text{O}_8$ (second cycle).

agreement with that obtained from the charge–discharge cycle test.

4. Conclusions

In summary, boron was doped into LiV_3O_8 through an aqueous solution reaction followed by heating at 100°C . The as-prepared materials were well characterized. The boron doping increases the interlayer spacing of materials structure and makes the materials structure more stable during charge–discharge cycles, which improve the electrochemical performance of LiV_3O_8 significantly. The reason for the good performance is that boron broadens the pathway between adjacent vanadate chains for the diffusion of lithium in the material and stabilizes the layer structure.

Acknowledgements

This work was financially supported by the National Science Fund for Outstanding Young Scientists of China (No. 50625207) and sponsored by the National Post Doctoral Fund of China.

References

- [1] A.L. Xie, C.A. Ma, L.B. Wang, Y.Q. Chu, *Electrochim. Acta* 52 (2007) 2945.
- [2] J.X. Dai, S.F. Li, Z.Q. Gao, K.S. Siow, *J. Electrochem. Soc.* 145 (1998) 3057.
- [3] G.Q. Liu, C.L. Zeng, K. Yang, *Electrochim. Acta* 47 (2002) 3239.
- [4] A.M. Kannan, A. Manthiram, *J. Power Sources* 159 (2006) 1405.
- [5] G. Yang, G. Wang, W.H. Hou, *J. Phys. Chem. B* 109 (2005) 11186.
- [6] Q.Y. Liu, H.W. Liu, X.W. Zhou, C.J. Cong, K.L. Zhang, *Solid State Ionics* 176 (2005) 1549.
- [7] S.V. Pouchko, A.K. Ivanov-Schitz, T.L. Kulova, A.M. Skundin, E.P. Turevkaya, *Solid State Ionics* 151 (2002) 129.
- [8] J.G. Xie, J.X. Li, H. Zhan, Y.H. Zhou, *Mater. Lett.* 57 (2003) 2682.
- [9] H.Y. Xu, H. Wang, Z.Q. Song, Y.W. Wang, H. Yan, M. Yoshimura, *Electrochim. Acta* 49 (2004) 349.
- [10] T.J. Patey, S.H. Ng, R. Büchel, N. Tran, F. Krumeich, J. Wang, H.K. Liu, P. Novák, *Electrochim. Solid-State Lett.* 11 (2008) A46.
- [11] N. Kosova, E. Devyatkina, *Mechanochem. Mech. Alloy.* 39 (2003) 5031.
- [12] N. Kumagai, Y.U. Aishui, *J. Electrochem. Soc.* 144 (1997) 830.
- [13] G. Pistoia, G. Wang, D. Zane, *Solid State Ionics* 76 (1995) 285.
- [14] M. Pasquali, G. Pistoia, *Electrochim. Acta* 36 (1991) 1549.
- [15] S.V. Pouchko, A.K. Ivanov-Schitz, T.L. Kulova, A.M. Skundin, E.P. Turevkaya, *Solid State Ionics* 151 (2002) 129.
- [16] M. Zhao, L.F. Jiao, H.T. Yuan, Y. Feng, M. Zhang, *Solid State Ionics* 178 (2007) 387.
- [17] C.Q. Feng, L.F. Huang, Z.P. Guo, J.Z. Wang, H.K. Liu, *J. Power Sources* 174 (2007) 548.
- [18] L. Liu, L.F. Jiao, J.L. Sun, M. Zhao, Y.H. Zhang, H.T. Yuan, Y.M. Wang, *Solid State Ionics* 178 (2008) 1756.
- [19] C.Q. Feng, S.Y. Chew, Z.P. Guo, J.Z. Wang, H.K. Liu, *J. Power Sources* 174 (2007) 1095.
- [20] S.Y. Chew, C.Q. Feng, S.H. Ng, J.Z. Wang, Z.P. Guo, H.K. Liu, *J. Electrochem. Soc.* 154 (2007) A633.
- [21] S. Jouanneau, A.L. Salle, A. Verbaere, M. Deschamps, S. Lascaud, D. Guyomard, *J. Mater. Chem.* 13 (2003) 921.
- [22] V. Manev, A. Momchilov, A. Nassalevska, G. Pistoia, M. Pasquali, *J. Power Sources* 54 (1995) 501.
- [23] J. Kawakita, T. Kato, Y. Katayama, T. Miura, T. Kishi, *J. Power Sources* 81–82 (1999) 448.
- [24] E.P. Koval' chuk, O.V. Reshetnyak, Y.S. Kovalyshyn, J. Błażejowski, *J. Power Sources* 107 (2002) 61.
- [25] Y.J. Wei, C.W. Ryu, K.B. Kim, *J. Power Sources* 165 (2007) 386.